Ignition of a Safran's Helicopter Engine With a Compact Nanosecond Laser System

Martin Maillard, Gabriel Amiard Hudebine, Mikael Orain, Pierre Doublet, Patrick Beaures d'Augères, Claude Bérat, Christophe Viguier, Stéphane Douillard, Eric Freysz

IGNITION OF A SAFRAN'S HELICOPTER ENGINE WITH A COMPACT NANOSECOND LASER SYSTEM

Martin MAILLARD[1,2], Gabriel AMIARD-HUDEBINE[2], Mikaël ORAIN[1], Pierre DOUBLET[1], Patrick BEAURE-D'AUGERES[3], Claude BERAT[4], Christophe VIGUIER[4], Stéphane DOUILLARD[4] and Eric FREYSZ[2]

[1]ONERA/DMPE, Université de Toulouse, 31055 Toulouse, France
[2]Univ. Bordeaux, CNRS, LOMA, UMR 5798, F-33400 Talence, France
[3]Fibercryst, 69150 Décines-Charpieu, France
[4]Safran Helicopter Engines, 64510 Bordes, France

ABSTRACT

We report on the ignition of a Safran's helicopter engine using a compact laser system. The laser system delivers nanosecond infrared pulses at a high repetition rate which energy can be up to 40mJ. *The first tests were run on a Safran Helicopter Engines experimental bench operating at room temperature and ambient pressure with jet A-1 fuel. We studied in detail the impact of the laser pulse energy and the spark position on the engine ignition domain. An optical focusing system fixed on the engine casing enables to focus the laser pulse at different positions in the combustion chamber. The focused laser beam generates a plasma in the combustion chamber, which ignites the engine. Our experimental data show that the laser spark position impacts the pulse energy required to ignite the engine. At the optimal position, we very reliably ignite the engine with a pulse energy of only* 3mJ. *To understand this behavior, similar experiments were run on the MERCATO experimental bench at ONERA (the French aerospace lab). This bench faithfully reproduces the geometry and the flow field of the Safran engine's combustion chamber. Using a Mie scattering imaging technique, we studied the kerosene spray generated by the start injector. Our data indicates that depending on the laser spark position in the combustion chamber, the kerosene droplets scatter more or less the laser light. This impacts the pulse energy and its spot size at the focal point and influences the laser ignition probability. In addition, ignition success requires a minimum density of kerosene droplets. Hence, the optimal laser spark position is a compromise between the droplet density at the focal point and the laser beam scattering induced by droplets before reaching that position.*

1. INTRODUCTION

Over the years, ignition of aeronautic engines has consistently been obtained using conventional spark plugs, which yet exhibit many drawbacks (ignition close to the combustor walls, spark erosion, low repetition rate of the spark, etc.) [1]. As a result, alternative ignition systems with improved performances have triggered a lot of interest. Examples include plasma igniters, microwave-based systems, laser sources, etc. [2–7]. Laser ignition has been shown to limit the main drawbacks of spark plug ignition and presents many advantages [8–10]. For instance, the repetition rate of the laser source is significantly higher than that of the spark igniter(about100Hzversus0.5-3Hz). Besides, laser ignition makes it is possible to locate the ignition kernel at any position within the combustion chamber. Different laser ignition techniques have been proposed such as thermal ignition [11, 12], photo-chemical ignition [13, 14], resonant breakdown [15, 16], non-resonant breakdown [8,17]. The latter is the most convenient laser technique to ignite an engine [10, 18–20]. It relies on the fact that when one focuses an energetic infrared nanosecond laser pulse in air, it ionizes it, giving rise to an electron avalanche which induces plasma breakdown in air. This plasma spark leads to the development of a rapidly expanding shock wave which ignites the fuel-air mixture [17]. While the development of laser technologies makes this technique very attractive [18, 21, 22], only few experimental studies have been dedicated to laser ignition of liquid fuel/air mixtures [23–30]. Hence, with no surprise and to the best of our knowledge, no laser ignition of an aeronautic engine has so far been reported. Hereafter, we demonstrate that a nanosecond laser pulse focused in a Safran aeronautic engine can very easily ignite it. When the laser spark is properly located in the combustion chamber, a nanosecond pulse with an energy of only 3mJ is needed to ignite the engine at room temperature and ambient pressure operating with Jet A-1 liquid fuel. We also evidence that the optimal location of the laser sparks in the combustion chamber depends of the kerosene droplets density and the scattering of the laser pulse by kerosene spray.

2. LASER IGNITION OF A SAFRAN'S HELICOPTER ENGINE

2.1 Experimental setup

In January 2022, we carried out a laser ignition test campaign on a Safran's helicopter engine with a compact laser source. As for all new ignition system, we had to define the relevant ignition domain which indicates conditions (both flow and laser conditions) where ignition is very likely to occur. To define it, we measure the evolution of engine ignition versus the laser pulse energy and the laser spark position (Z_{LSP}) within the engine combustion chamber (CC). Figure 1 displays the experimental setup used.

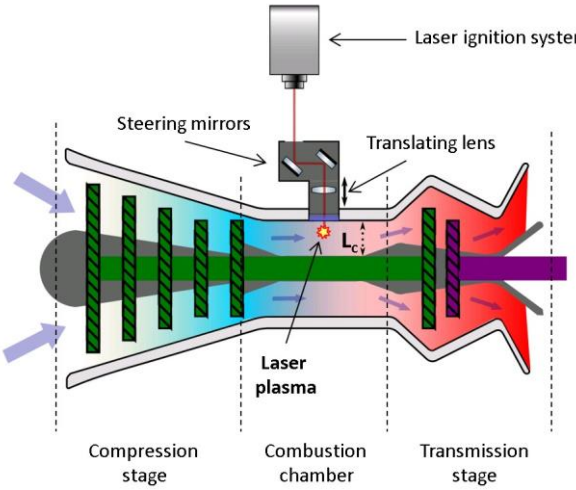

Figure 1: Sketch of the setup used to laser ignite the Safran's helicopter engine.

Ignition of the aeronautic engine is performed with a homemade Master Oscillator Power Amplified (MOPA) Nd:YAG system specially designed to deliver at high frequency (~ 100 Hz), ~ 1 ns pulses centered at 1.064µm which energy per pulse can be up to 40mJ. Importantly, a big deal of efforts was dedicated to ensure the laser beam has a $M^2 \sim 1.2$. The laser energy deposition in the plasma is a well-known phenomenon, it is about 30% of the incident laser pulse energy [31]. The conventional spark plug of the engine is removed and a sapphire window is installed to keep the CC sealed. At the location of the conventional spark plug, we fixed an optical system which enables to focus the laser pulse at Z_{LSP} in the CC. The latter is normalized according to the CC height. The laser spark position (LSP) can be adjusted in between 0% (wall of the CC) and 41%. At the LSP, the laser pulse ionizes air and generates a spark which ignites the droplets of kerosene (Jet A-1) dispersed in air. Thanks to the M^2 of the laser beam, at the focal point the beam diameter is small (~ 10µm) and the volume within the confocal distance is about 2.4×10^{-14} m^3. The experiments are run at room temperature ($0°C<T_a<20°C$) and atmospheric pressure (P_a). The ignition procedure is as follows: as the laser fires pulses which energy and LSP are set, the starter accelerates the engine during ~10 s, up to 20% of its nominal speed while kerosene is injected in the CC. If the ignition is successful, the engine is stopped before it reaches its nominal speed and then cooled down for about half an hour.

The influence of the LSP on the ignition domain is determined by searching the minimum ignition energy (MIE) required to ignite the CC at different spark positions. The better the LSP, the lower the laser pulse energy. Therefore, at each position, we start with a high laser energy (about 20 mJ) and then, we gradually decrease the energy until the ignition fails. Then, we get back to the previous pulse energy to check our ability to ignite the engine at least twice in a row. A second successful ignition confirms we reached the MIE at this position.

2.2 Results

Figure2 displays the MIE evolution versus the LSP in the CC. The red curve indicates the limit of the ignition domain colored in green. This figure underlines that the laser pulse energy is crucial. Indeed, whatever the LSP, we cannot ignite the engine when the laser pulse energy is below 3mJ. However, the spark position has a tremendous impact on the MIE. Near the CC wall (LSP<5%), the MIE is about 20mJ. As the LSP increases, the MIE decreases down to 3mJ for Z_{LSP} = 27% and then slightly increases up to 5mJ at Z_{LSP} = 41%. In order to understand this behavior, we performed further laser ignition experiments on a scale model

of the Safran's helicopter engine CC at ONERA (The French aerospace lab), which allows to carry out parametric ignition studies at reduced costs compared to tests on a real engine.

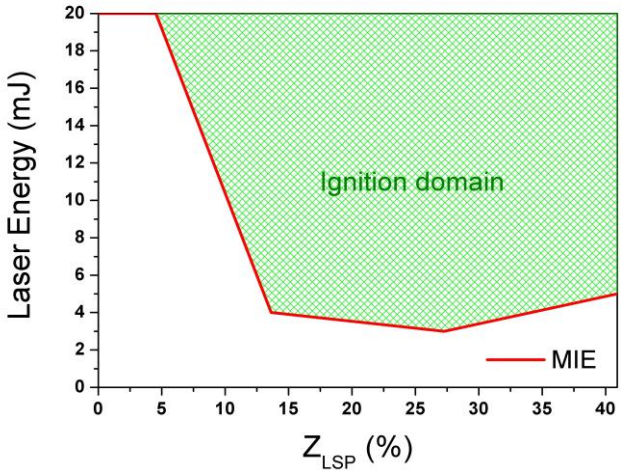

Figure 2: Laser spark plug ignition domain on the Safran's helicopter engine.

3. LASER IGNITION ON A SCALE MODEL OF AN HELICOPTER COMBUSTION CHAMBER

3.1 MERCATO bench

The MERCATO [32] test facility, located at ONERA/Le Fauga-Mauzac, is an air-breathing propulsion research facility dedicated to ignition and spray investigations. It can reproduce temperatures (fuel and air) and pressures in the range [40, +20] °C and [0.3, 1] bar (abs) respectively, which is representative of cold start or altitude relight. It can be operated with Jet A-1 kerosene or Sustainable Alternative Fuels (SAF). Both air and fuel mass flow rates are measured by Coriolis flow meters and regulated by valves. Sub-atmospheric pressure in the CC is classically obtained by means of a supersonic ejector. For the present experiments, the MERCATO facility is equipped with a scale model of the Safran's helicopter engine CC which accurately reproduce the ignition performances of a complete Safran's CC under various conditions, at low air flow rate when it starts or at high air flow rate when it needs to be reignited.

3.2 Experimental setup

Figure 3 sketches the MERCATO experimental bench. Similarly, to the experiments performed at Safran Helicopter Engines, we used the same laser, focusing system and starting injector. This injector provides a full cone of droplets which average Sauter mean diameter is ~ 25 µm. To ignite the combustor, the conventional spark plug is removed, the CC is sealed with a sapphire window and the conventional spark plug is replaced by the optical system which focuses the laser pulses in the CC. For the laser ignition experiments run on the MERCATO bench, fuel mass flow rate is set constant while pressure in the CC varies between 0.4 bar and atmospheric pressure, at ambient temperature. Thanks to a beam shutter set on the laser beam path, laser ignition is only performed when air and fuel mass flow rates are at a steady state in the combustor. To image the fuel spray distribution in the combustor, we use a Mie scattering method [33]. It consists of a high-speed laser system (Darwin 527-30 from Quantronix) delivering laser pulses at 527 nm (energy about 15 mJ, pulse duration 200 ns, repetition rate 2 kHz). Using spherical and cylindrical lenses, the laser beam is transformed into a thin laser sheet (e_{sheet} ~ 1 mm) which is sent into the CC. The laser sheet propagates along the ignition laser axis and illuminate the droplet spray on the injector axis. Mie scattering from droplets is recorded at right angles from the laser sheet with a high-speed CMOS camera (VEO 710 from Phantom) which is equipped with a Notch filter centered at 532 nm (FWHM 18 nm). The camera resolution is about 50 µm per pixel. The camera and the laser are synchronized using a signal generator triggered by the shutter opening.

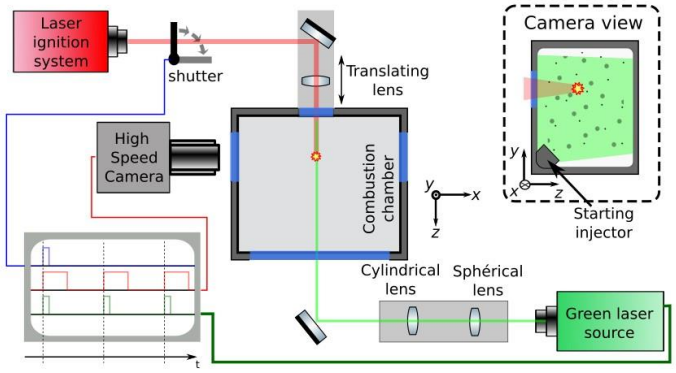

Figure 3: Schematic of the combustor ignition bench monitored with a Mie Scattering setup.

3.3 Results

The aim of these experiments is to determine the ignition domain versus the LSP inside the CC and the air mass flow rate. The latter is normalized against the nominal air mass flow rate used with a conventional spark plug. To perform the experiments, the laser beam energy is set at its maximum (~ 40 mJ) and we characterize the combustor ignition performances (success or failure) as a function of the air mass flow rate for each LSP. For a given operating condition (air and fuel temperature, combustor pressure), ignition performance tests consist in searching the highest air mass flow rate that leads to successful stabilized combustor ignition. So, the highest the air mass flow rate we can ignite, the better the ignition system. The procedure to determine the air mass flow rate limit of ignition is the following. We begin the ignition test with a high air mass flow rate and reduce it until we succeed to ignite. Then, we wait for 15 minutes for the combustor to cool down. We repeat this procedure three time to guarantee that the ignition occurs always with the same air flow rate limit.

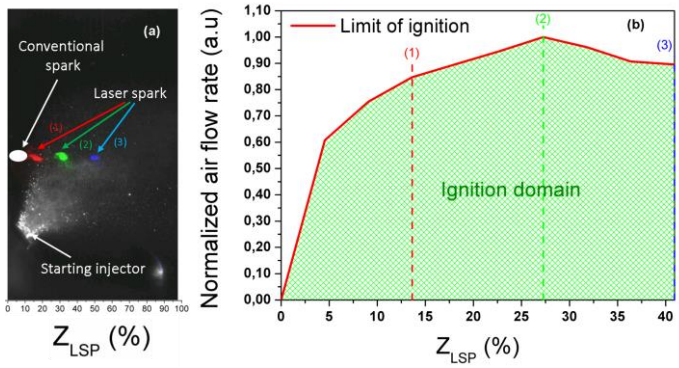

Figure 4: (a) Image acquired by the high-speed camera: the starting injector is located at the bottom left of the image and the different positions of the laser spark are represented by colored circles. (b) Ignition domain is displayed in green. It is plotted versus the laser spark position Z_{LSP} in the combustor and the normalized air mass flow rate at ambient pressure Pa and room temperature T_a.

The Fig.4(a) displays a superposition of images recorded by the camera. It shows the kerosene spray pattern, the position of the plasma of the conventional spark plug and the laser-induced spark located at different positions in the combustor. This image highlights the ability of a laser system to deposit energy (to generate a plasma) at positions inside the combustion chamber that cannot be reached by conventional spark plugs. Figure 4(b) displays the laser ignition domain versus the air mass flow rate. The colored lines numbered (1), (2) and (3) pinpoint the three laser spark positions highlighted in red, green and blue in Fig.4(a), respectively. In very good agreement with the results obtained in the Safran's helicopter engine, we observe that the closer the laser spark to the wall (Z_{LSP} < 5%), the lower the ignition domain. As we move the LSP further in the combustor, the ignition domain rapidly increases and it is optimal when Z_{LSP} ~ 27%.

4. INFLUENCE OF THE DROPLET SPRAY ON THE LASER IGNITION

Hereafter, we study the spray evolution versus pressure and air mass flow rate in the combustor. We present their impact on the spray angle as well as on the droplet size and spatial distribution.

4.1 Relation between the air mass flow rate and the spray angle

Figure 5 displays the spray angle normalized against its maximum value. We define the spray angle as the angle of a cone that includes 95% of the detected droplets. Figure 5 indicates that the pressure does not notably impact the evolution of the spray angle as a function of the air mass flow rate. However, it shows that there is a linear relationship between the spray angle and the air mass flow rate. Hence, at high flow rate, little kerosene droplets are located near the combustor wall, which considerably reduces the probability to generate a flame kernel and subsequently the ignition probability of the CC. This phenomenon clearly evidences the advantage of a laser ignition system versus the conventional spark plug which spark is mostly located near the combustor wall. With a laser ignition system, one can locate the spark farther from the combustor wall, enhancing the probability to generate a flame kernel, reducing its quenching by the combustor wall and thus increasing our ability to ignite the engine.

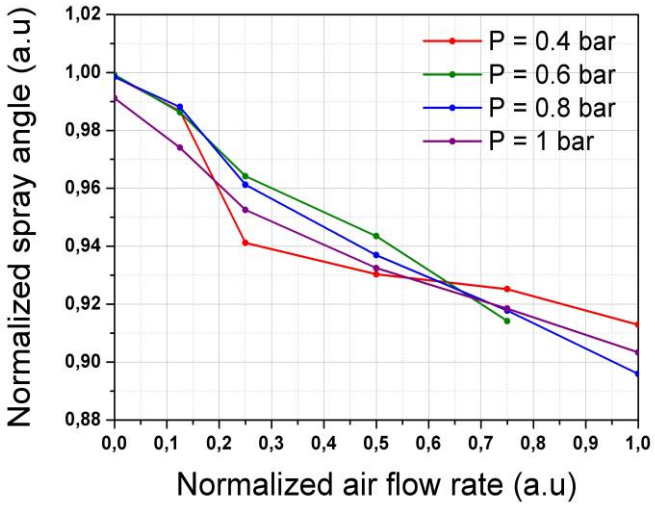

Figure 5: Evolution of the spray angle versus the normalized air mass flow rate.

Figure 5 displays the spray angle normalized against its maximum value. We define the spray angle as the angle of a cone that includes 95% of the detected droplets. Figure 5 indicates that the pressure does not notably impact the evolution of the spray angle as a function of the air mass flow rate. However, it shows that there is a linear relationship between the spray angle and the air mass flow rate. Hence, at high flow rate, little kerosene droplets are located near the combustor wall, which considerably reduces the probability to generate a flame kernel and subsequently the ignition probability of the CC. This phenomenon clearly evidences the advantage of a laser ignition system versus the conventional spark plug which spark is mostly located near the combustor wall. With a laser ignition system, one can locate the spark farther from the combustor wall, enhancing the probability to generate a flame kernel, reducing its quenching by the combustor wall and thus increasing our ability to ignite the engine.

4.2 Study of the droplet density and droplet inter-distance versus the laser spark position

In an attempt to explain why the optimal LSP is around 27% of the combustor height, we need to study in more details the droplet density and the droplet inter-distance (d_{id}) along the LSP range. The droplet inter-distance corresponds to the distance of a droplet to its nearest neighbor. In order to derive these parameters from the Mie scattering images, we use a method similar to that previously developed by Rousseau et al. [33]. The Figure 6 represents the different steps of the processing.

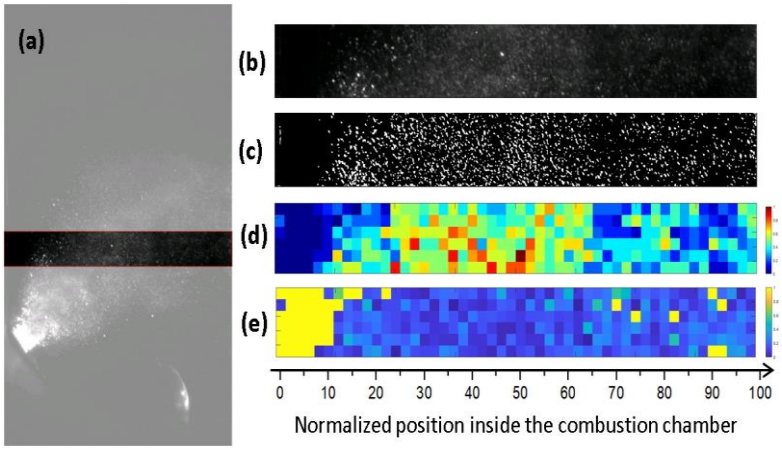

Figure 6: Image processing methods. (a) ROI position in a Mie scattering image. (b) Cropped image of the ROI. (c) Binarization process to identify the droplets. (d) Averaged map of the normalized droplet density. (e) Averaged map of the normalized inter-droplet distance.

The algorithm runs as follows: we extract the droplets from the background and then compute the droplet density and d_{id}. In order to reduce the computation time, we focus our analysis of the images (Fig.6(a)) on the region of interest (ROI) in dark along the propagation axis of the ignition laser pulse in the combustor, which yields the cropped image displayed in Fig.6(b). On this cropped image, we apply a combination of successive morphological dilatation and arithmetic operations that better segregate the droplets and extract their contours. Since we consider the droplets to behave as disk elements, we use a disk-shaped structuring element to run this procedure. We further apply a binarization operation on the gray scale image. In order to work properly, this algorithm requires a careful choice of two parameters. The first one is the radius (r_{disk}) of the disk-shaped element while the second one is the threshold value (h_{th}) used to perform the binarization operation. To choose these parameters, we run a parametric study and test values of r_{disk} between 1 and 3 pixels and of h_{th} between 0 and 4095. For our optical configuration, the best couple of parameters avoiding false droplet detection coming from the merging of droplets or from multi-scattering effects is r_{disk} = 1 pixel and h_{th} = 2000. The Fig.6(c) presents the results of such a computation. On these binary images, we further perform a blob analysis during which a labeling function identifies each droplet and generates lists of droplets' barycenter coordinates. Then, we use these lists to compute the droplet density and d_{id}. To perform these latter computations, we divide our cropped image in meta-pixels, a meta-pixel being composed of 24 × 24 pixels. This considerably reduces the computation time, further smooths the images and accordingly drastically reduces the noise. Thanks to the labeling function, we can list all the droplets within each meta-pixel and derive the corresponding droplet density within a meta-pixel which writes:

$$D_{meta-pixel} = \frac{N_{meta-pixel}}{S_{meta-pixel} e_{laser}}$$

where $D_{meta-pixel}$ is the droplet density in a meta-pixel, $N_{meta-pixel}$ is the number of droplets within the meta-pixel, $S_{meta-pixel}$ is the surface of a meta-pixel and e_{laser} is the thickness of the laser sheet. The Fig.6(d) displays the normalized droplet density map. As expected, and in agreement with Fig.6(a), the density is very low near the wall. It gradually increases and then remains almost constant when the LSP is between 20% and 60%. When the LSP is above 60%, the droplet density decreases.

To compute the evolution of the d_{id} in the combustor, we average d_{id} on a meta-pixel. For each droplet j in a meta-pixel, d_{id} writes:

$$d_{id,j} = min\left(\sqrt{(x_i - x_j)^2 + (y_i - y_j)^2}\right),$$
$$\forall\, i \in [1, N_{meta-pixel}]\ and\ i \neq j$$

with ($x_{i,j}$, $y_{i,j}$) the barycenter coordinates of the droplet i and j respectively. Hence d_{id} writes:

$$d_{id} = \frac{1}{N_{meta-pixel}} \sum_{j=1}^{N_{meta-pixel}} d_{id,j}$$

The Fig.6(e) displays the d_{id} map. Near the wall, the d_{id} value is very high as there are only few droplets. As the laser pulse further propagates in the combustor, d_{id} lowers and finally remains constant.

The Fig. 7 displays the result of image processing performed over a sequence of 500 instantaneous images when the LSP ranges between 0% and 41%. This result highlights why it is more difficult to ignite the fuel/air mixture when the laser spark is near the wall. Indeed, near the combustor wall, the droplet density is very small, making a flame kernel generation difficult. The latter can be very easily quenched by the combustor wall, making the engine ignition very difficult [34]. As the laser spark is moved further towards the center of the combustor, the droplet density rises. It is about its nominal value when the LSP is above 25%. Afterwards, the droplet density and d_{id} remains quasi-constant along the axis. Accordingly, in a first approach, the ignition domain should remain almost constant when the LSP is between 20% and 41%, which is at variance with our experimental results. We address the issue in the next part.

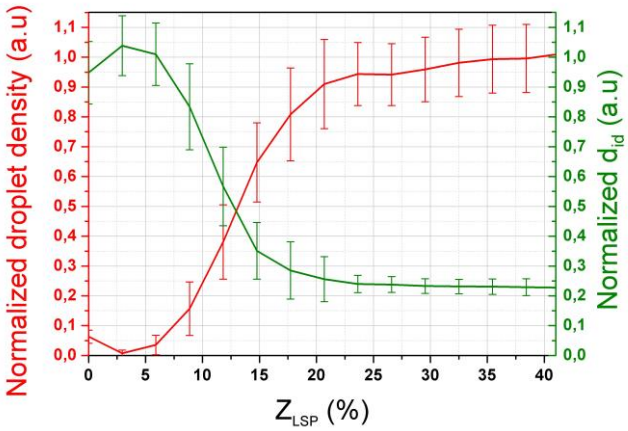

Figure 7: Spray characteristics prior to the ignition. The red curve displays the droplet density normalized by its maximum value and the green curve displays d_{id} normalize by its maximum value.

5. DISCUSSION

As mentioned previously, the low ignition capability of the laser system when the spark is located near the combustor wall can be easily explained. However, to better understand why the optimal LSP is around 27%, one can, as often, mention the recirculation in the flame kernel within the combustor [35, 36]. But besides this phenomenon, it is also necessary to account for the beam propagation in the CC before reaching the focal point. Indeed, as the beam propagates, before reaching the LSP, the laser pulse can be scattered by the kerosene droplets. This scattering lowers the laser pulse energy and creates wave-front distortion of the laser beam profile introducing aberrations at LSP. The higher the aberrations, the lower the beam focusing, and therefore, the higher the confocal volume. This results in lowering the power density at the LSP and, subsequently, the kernel ignition temperature. Evaluating the impact of the droplet scattering on ignition capabilities requires to evaluate both energy losses and laser beam aberration. It is worth noting that depending on the position of the droplets along the beam propagation axis, the beam diameter varies from several orders of magnitude larger to about the size of a droplet. Near the focal point, the laser energy density is very high inducing multi-photonic absorption inside kerosene droplets. This leads to heating and evaporation of the droplets, which modifies their refractive index and further influences the laser beam propagation [37]. As a result, the aberrations and scattering drastically vary along the beam path. For a spatially Gaussian beam, it also depends on the radial position with respect to the beam axis. Therefore, evaluating the kerosene droplets impact on the scattering and wavefront distortion of Gaussian laser beam within the combustion chamber requires a dedicated study, which is out of the scope of the present paper. In any case, it is obvious that the lower the number of scattering events, the better the ignition. Using simple analysis, we can evaluate the number of scattering events. Let us consider that the laser beam has a perfect Gaussian shape. As it propagates, the beam size $\omega(z)$ along the z propagation axis writes:

$$\omega(z) = \omega_0 \sqrt{1 + \left(\frac{\lambda(z - z_{LSP})}{\pi\omega_0^2}\right)^2}$$

where ω_0 and λ are the radius of the beam at the focal point and the laser wavelength, respectively. Figure 8 displays the beam radius $\omega(z)/\omega_0$ focused at 14% (red), 27% (green) and at 41% (blue) position of the

combustor, respectively. It is worth noting the higher the LSP, the larger the laser beam volume within the combustor.

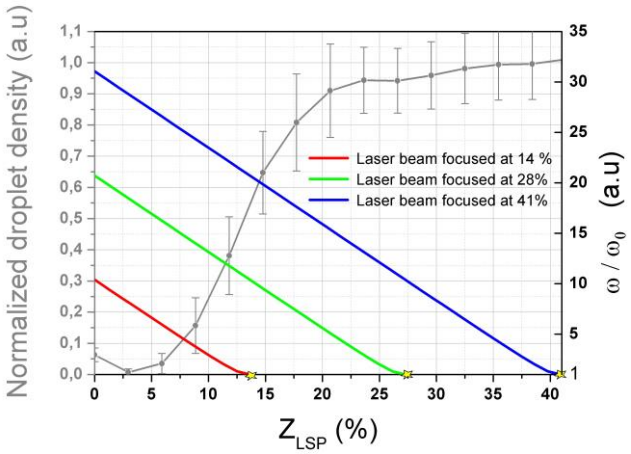

Figure 8: Comparison between the laser beam size and the ignition domain. The gray curve displays the Normalized droplet density. The red, green and blue curves display respectively the evolution of the normalized laser beam radius when it is focused respectively at 14 %, 27 % and 41 %.

We evaluate the number of scattering droplets N_{sc} seen by the laser pulse before it reaches Z_{LSP}. It writes:

$$N_{sc} = \int_0^{Z_{LSP}} \pi\omega^2(z) Z_{LSP} D(z) dz$$

where $D(z)$ is the droplet density along the laser beam axis (Fig.8, black curve). Figure 9 displays the evolution of N_{sc} versus Z_{LSP}. N_{sc} increases almost exponentially with respect to Z_{LSP}. At the position Z_{LSP} = 41 %, N_{sc} is ~ 18 whereas it is only ~ 4 for Z_{LSP} = 27% (the optimal position). This indicates that the optimal position for the laser spark is a compromise between the droplet density at the focal point and the scattering of the laser beam before the LSP.

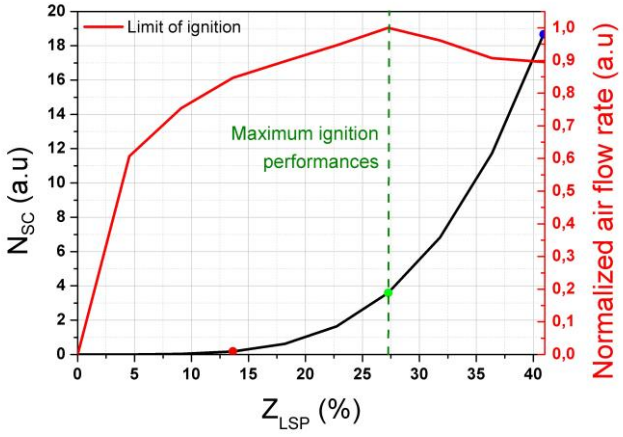

Figure 9: Comparison between the ignition domain and the number of droplets that scatter the laser beam. The red curve displays the limit of air mass flow rate ignition and the black curve displays the number of droplets that scatter the laser beam versus the laser spark position.

6. CONCLUSION

For the first time, to our best knowledge, a helicopter engine was ignited at ambient temperature and atmospheric pressure by a laser spark plug at Safran Helicopter Engines facilities. Thanks to an adjustable

focusing system, we were able to study the influence of the laser spark position on the ignition domain of the engine. It appears that there is an optimal position of Z_{LSP} at 27% where we very reliably ignite the engine with infrared nanosecond pulses which energy is only 3mJ. The latter is about one or two orders of magnitude lower than the energy used previously to ignite air kerosene mixture [30]. This energy was confirmed on a scale model of the Safran engine CC on the MERCATO test bench at ONERA. On this bench and thanks to a Mie scattering imaging method, we were able to demonstrate that at this optimal position, the density of kerosene droplets is the highest while laser scattering remains weak. This enhances the probability to create a viable flame kernel which ignites the engine. This work offers many prospects. In a forthcoming paper, we will report on the successful laser ignition experiments we performed on the ONERA's MERCATO bench varying temperature (down to -40 °C) and pressure (down to 0.4 bar). These new results will demonstrate our laser system outperforms the conventionally used spark plugs. In fact, laser ignition can bypass most of the problems encountered by conventional spark plugs such as low discharge repetition rate or position of flame kernel close to the engine wall which can be easily quenched. So far, the design of the combustion chamber has taken into account these limitations. Most of them will be easily relaxed using laser ignition. Even if lasers bring their own constraints related to their higher cost and their optimal working temperature, they open new possibilities that have yet to be imagined and tested.

ACKNOWLEDGMENTS

This work was partly supported by the "Conseil Régional Nouvelle-Aquitaine" and the "Agence Nationale de la Recherche (LAMA, ANR-18-ASMA-0004-01)". M.M., G.A.-H., M. O and E.F. thank the team operating the Safran Helicopter Engines bench for their suggestions and help during the ignition experiments ran at Bordes.

REFERENCES

[1] Moesl, Klaus G, Vollmer, Klaus G, Sattelmayer, Thomas, Eckstein, Johannes and Kopecek, Herbert. "Experimental Study on Laser-Induced Ignition of Swirl-Stabilized Kerosene Flames." Vol. 43130 (2008): pp. 383–392.

[2] Starikovskiy, Andrey and Aleksandrov, Nickolay. "Plasma assisted ignition and combustion." *Progress in Energy and Combustion Science* Vol. 39 No. 1 (2013): pp. 61–110.

[3] Michael, James B, Chng, Tat Loon and Miles, Richard B. "Sustained propagation of ultra-lean methane/air flames with pulsed microwave energy deposition." *Combustion and Flame* Vol. 160 No. 4 (2013): pp. 796–807.

[4] Jose, Jubin Vand Sreenath, VR. "Review on performance of high energy ignition techniques." *International Journal of Research and Innovations in Science and Technology* Vol. 2 No. 2 (2015).

[5] Lovascio, Sara, Hayashi, Jun, Stepanyan, Sergey, Stancu, Gabi D and Laux, Christophe O. "Cumulative effect of successive nanosecond repetitively pulsed discharges on the ignition of lean mixtures." *Proceedings of the Combustion institute* Vol. 37 No. 4 (2019): pp. 5553–5560.

[6] Lin, Bing-xuan, Wu, Yun, Xu, Ming-xing and Chen, Zhigang. "Experimental investigation on spark ignition and flame propagation of swirling kerosene spray flames." *Fuel* Vol. 303 (2021): p. 121254.

[7] Lin, Bing-xuan, Wu, Yun, Xu, Ming-xing and Shen, Yanming. "Experimental Investigation on High-Altitude Ignition and Ignition Enhancement by Multi-Channel Plasma Igniter." *Plasma Chemistry and Plasma Processing* Vol. 41 No. 5 (2021): pp. 1435–1454.

[8] Ronney, Paul D. "Laser versus conventional ignition of flames." *Optical Engineering* Vol. 33 No. 2 (1994): pp. 510–521.

[9] Weinrotter, Martin, Kopecek, Herbert, Wintner, Ernst, Lackner, Maximilian and Winter, Franz. "Application of laser ignition to hydrogen–air mixtures at high pressures." *International journal of hydrogen energy* Vol. 30 No. 3 (2005): pp. 319–326.

[10] Phuoc, Tran X. "Laser-induced spark ignition fundamental and applications." *Optics and Lasers in Engineering* Vol. 44 No. 5 (2006): pp. 351–397.

[11] Hill, RA and Laguna, GA. "Laser initiated combustion of CH4+ O2 mixtures." *Optics Communications* Vol. 32 No. 3 (1980): pp. 435–439.

[12] Li, Xiaohui, Yu, Xin, Fan, Rongwei, Yu, Yang, Liu, Chang and Chen, Deying. "Laser ablation ignition of premixed methane and oxygen-enriched air mixtures using a tantalum target." *Optics Letters* Vol. 39 No. 1 (2014): pp. 139–141.

[13] Lavid, Moshe and Stevens, John G. “Photochemical ignition of premixed hydrogenoxidizer mixtures with excimer lasers.” *Combustion and Flame* Vol. 60 No. 2 (1985): pp. 195–202.

[14] Chou, Mau-Song and Zukowski, Tmitri J. “Ignition of H2/O2/NH3, H2/air/NH3 and CH4/O2/NH3 mixtures by excimer-laser photolysis of NH3.” *Combustion and Flame* Vol. 87 No. 2 (1991): pp. 191–202.

[15] Forch, Brad E and Miziolek, Andrzej W. “Oxygen-atom two-photon resonance effects in multiphoton photochemical ignition of premixed H 2/O 2 flows.” *Optics letters* Vol. 11 No. 3 (1986): pp. 129–131.

[16] Forch, Brad E. “Resonant laser ignition of reactive gases.” *Laser Applications in Combustion and Combustion Diagnostics II*, Vol. 2122: pp. 118–128. 1994. SPIE.

[17] Bradley, D, Sheppard, CGW, Suardjaja, IM and Woolley, R. “Fundamentals of high-energy spark ignition with lasers.”
Combustion and Flame Vol. 138 No. 1-2 (2004): pp. 55–77.

[18] Morsy, Mohamed H. “Review and recent developments of laser ignition for internal combustion engines applications.” *Renewable and Sustainable Energy Reviews* Vol. 16 No. 7 (2012): pp. 4849–4875.

[19] Börner, Michael, Manfletti, Chiara, Kroupa, Gerhard and Oschwald, Michael. “Laser ignition of an experimental combustion chamber with a multi-injector configuration at low pressure conditions.” *CEAS Space Journal* Vol. 9 No. 3 (2017): pp. 299–311.

[20] Pavel, Nicolaie, Croitoru, Gabriela, Grigore, Oana-Valeria,
Vasile, Nicolae-Tiberius, Dascalu, Traian, Birtas, Adrian, Boicea, Nicolae, Dinca, Mihai, Draghici, Florin and Chiriac, Radu. “Laser spark-plug development: from experimental device to successful engine ignition.” *Advances in 3OM: Opto-Mechatronics, Opto-Mechanics, and Optical Metrology*, Vol. 12170: pp. 185–192. 2022. SPIE.

[21] Dearden, Geoff and Shenton, Tom. “Laser ignited engines: progress, challenges and prospects.” *Optics express* Vol. 21 No. 106 (2013): pp. A1113–A1125.

[22] O’Briant, Steven A, Gupta, Sreenath B and Vasu, Subith S. “Laser ignition for aerospace propulsion.” *Propulsion and Power Research* Vol. 5 No. 1 (2016): pp. 1–21.

[23] Tihay, Virginie, Gillard, Philippe and Blanc, Denis. “Ignition study of acetone/air mixtures by using laser-induced spark.” *Journal of hazardous materials* Vol. 209 (2012): pp. 372–378.

[24] Xu, Cangsu, Fang, Donghua, Luo, Qiyuan, Ma, Jian and Xie, Yang. “A comparative study of laser ignition and spark ignition with gasoline–air mixtures.” *Optics & Laser Technology* Vol. 64 (2014): pp. 343–351.

[25] Moesl, Klaus G, Vollmer, Klaus G, Sattelmayer, Thomas, Eckstein, Johannes and Kopecek, Herbert. “Experimental study on laser-induced ignition of swirl-stabilized kerosene flames.” *Journal of engineering for gas turbines and power* Vol. 131 No. 2 (2009).

[26] de Oliveira, Pedro M, Allison, Patton M and Mastorakos, Epaminondas. “Ignition of uniform droplet-laden weakly turbulent flows following a laser spark.” *Combustion and Flame* Vol. 199 (2019): pp. 387–400.

[27] Xu, Cang-su, Fang, Dong-hua, Luo, Qi-yuan, Ma, Jian, Xie, Yang and Zheng, Xu. “Characterization of gasoline combustion with laser and spark ignition.” *Journal of Zhejiang University-SCIENCE A* Vol. 16 No. 10 (2015): pp. 830–838.

[28] Oldenborg, Richard, Early, James and Lester, Charles. “Advanced ignition and propulsion technology program.” Technical report no. Los Alamos National Lab.(LANL), Los Alamos, NM (United States). 1998.

[29] Li, Mengzhe, Wang, Zhikai, Xu, Rongguang, Zhang, Xiaoliang, Chen, Zhitong and Wang, Qiu. “Advances in plasma-assisted ignition and combustion for combustors of aerospace engines.” *Aerospace Science and Technology* Vol. 117 (2021): p. 106952.

[30] Gebel, Gregor C, Mosbach, Thomas, Meier, Wolfgang and Aigner, Manfred. “Optical and spectroscopic diagnostics of laser-induced air breakdown and kerosene spray ignition.” *Combustion and Flame* Vol. 162 No. 4 (2015): pp. 1599– 1613.

[31] Phuoc, Tran and White, C.M. “Optical characterization of the laser-induced spark in air.” *Optical Diagnostics in Engineering* Vol. 5 (2001): pp. 13–26.

[32] Cochet, Alain, Bodoc, Virginel, Brossard, Christophe,
Dessornes, Olivier, Guin, Christian, Lecourt, Renaud, Orain, Mikaël and Vincent-Randonnier, Axem. “ONERA test facilities for combustion in aero gas turbine engines, and associated optical diagnostics.” *Aerospace Lab* No. 11 (2016): pp. 16–pages.

[33] Rousseau, Lola, Lempereur, Christine, Orain, Mikael, Rouzaud, Olivier and Simonin, Olivier. “Droplet spatial distribution in a spray under evaporating and reacting conditions.” *Experiments in Fluids* Vol. 62 No. 2 (2021): pp. 1–19.

[34] Poinsot, T, Haworth, D and Bruneaux, G. “Direct simulation and modeling of flame-wall interaction for premixed turbulent combustion.” *Combustion and Flame* Vol. 95 No. 1-2 (1993): pp. 118–132.

[35] Cordier, Matthieu, Vandel, Alexis, Cabot, Gilles, Renou, Bruno and Boukhalfa, AbdelakrimMourad. “Laser-induced spark ignition of premixed confined swirled flames.” *Combustion Science and Technology* Vol. 185 No. 3 (2013): pp. 379–407.

[36] Wang, Xiwei, Huang, Yong, Liu, Yunfeng and Sun, Lei. “Effect of the ignition location on lean light-off limits for a gas turbine combustor.” *Combustion and Flame* Vol. 245 (2022): p. 112295.

[37] Pokharel, Sagar, Tropina, Albina and Shneider, Mikhail. “Numerical Modeling of Laser Heating and Evaporation of a Single Droplet.” *Energies* Vol. 16 No. 1 (2022): p. 388.